

Laser printing of passive electrical components

Author: Jose Mendoza Carreño.

Advisor: J.M. Fernández-Pradas

Facultat de Física, Universitat de Barcelona, Diagonal 645, 08028 Barcelona, Spain.*

Abstract: Laser Induced Forward Transfer (LIFT) is used as a useful alternative to other ink printing techniques. Printing conductive materials with any geometry as desired gives us a degree of freedom in many fields of needs, such as microelectronics design. In this work silver nanoparticles ink is used and its resistivity is measured. First of all, the adequate scanning speed to get conductive lines must be known. In order to do that, a first printing with several speeds is done. It is observed that if the scanning velocity is fast enough, individual droplets are formed. However, by diminishing the velocity, the droplets get closer and closer until they form a straight line. Moreover, if the speed continues reducing, agglomerated material is formed. Next step is to determine the appropriate energy for printing. In order to get this, several droplets with different energies are printed. It is observed that, as the energy increases, the droplets lose their regular geometry and show as a splash. Furthermore, several lines are printed with different energies and their resistance have been measured, expecting a decreasing linear dependence, as more conductive material is added. Nevertheless, a much more complex dependence is obtained. Finally, once the parameters have been optimized, a fourth and last one printing of a maze pattern with many electrodes is done, with the objective to study the length-resistance dependence. Although a non-uniformity printing effect appears along the sample, the resistance increases linearly with length.

I. INTRODUCTION

Microelectronic techniques are developing nowadays exponentially because of the increasing necessity of much smaller electronic devices used in many important fields of our society, such as medicine or telecommunications. But it is not just to miniaturize devices, but to be able to have them upon any kind of substrate, such as plastics or glass. Moreover, technology is beyond planar devices, it is possible nowadays to bend circuits and introduce a new concept known as flexible electronics [1,2]. Although photolithography has been the most popular technique in microelectronics for quite a long time, it is not the most convenient one to achieve these objectives, as it is specially focused on silicon. The main reason is that UV light is used to change properties from our photoresin, but this radiation is enough energetic to change the plastic substrate properties, such as natural or synthetic polymers. This is why there is much more interest in printing techniques, as they allow printing in this kind of substrate without changing its properties. Another great advantage from direct printing techniques in front of photolithography is the absence of masks, as we can print any desired pattern. From printing techniques, such as Laser Induced Forward Transfer (LIFT), a resolution high enough is obtained with an easier and cheaper process, more likely to be done on an industrial scale. Using this kind of techniques, the range of materials susceptible to be printed is much larger. From organo-metallic dissolved compounds, to conductive polymers, nanoparticles, solid materials, etc. These topics have been developed in a very short time, and in this work we will focus on LIFT

technique [3] that is used to print silver nanoparticles ink on a glass substrate. The main reason of interest in the silver nanoparticles ink is that patterns with high conductivity and little conductive wires are obtained for different applications, as may be RFIDs, LEDs or transistors and many others. LIFT technique is based on the localized energy absorption of an E.M. field. A laser is used because of its facilities to change the energy beam as well as the focusing ability. The focalized beam over a substrate pushes and ejects material. This ejected material is not because of the light's linear momentum itself, but of the expansion of a created bubble that expands and pushes the adjacent material, leading to a difference in pressure and it expels the material in a jet form. An illustrating scheme is shown in **FIG. 1**, where the laser focalized in the glass-ink interface is absorbed and the bubble created expands and ejects material over the microscopic glass slides.

II. EXPERIMENTAL SETUP

The laser used is Nd:YAG with wavelength 1064 nm, pulse duration of 120 ns, repetition ratio of 1 kHz and a Gaussian intensity distribution with a diameter of 80 μm . Energy range used is between 0.1 mJ and 1 mJ. This measuring process is done using a thermopile to convert energy absorbed in heat, and this heat in a voltage difference. The laser is coupled to a deflecting mirror system to scan in two directions. After the mirrors the beam is focalized with an f-theta lens with focal length of 100 mm. The chosen transferred material is a commercial silver nanoparticles ink (Sigma-Aldrich 736481). The typical particles diameter is <50 nm, its density is 1.45 g/ml and its viscosity is

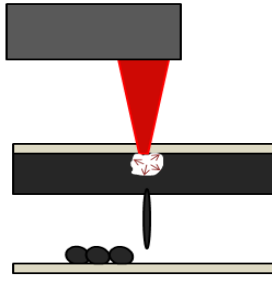


FIG. 1: LIFT scheme. The laser beam is focused on the donor film, where a bubble is created and expands, pushing away the material.

10-18 mPa·s. The substrates were microscopic glass slides (Deltalab, 76×26×1mm). Donor film is obtained by depositing 40 μ L into a clean side of the donor substrate spread with a blade into a surface of 50×26 approximately. Finally, the donor substrate is placed faced-down upon the acceptor substrate with a couple of 50 μ m separators. Once the pattern has been printed, it is still liquid and it must be dried and cured. The drying consists of putting the sample inside an oven until the ink becomes solid. This is done at a temperature of 50 °C to accelerate the process. The curing process consists of introducing the sample at a temperature of 200 °C during half an hour. The curing helps the coalescence between Ag nanoparticles to get a dense conductive media. The sample is observed in an optical microscope where the images are taken, as well as in a confocal microscope to extract line profiles. The resistance is measured with a standard multimeter.

III. RESULTS

First of all it is necessary to fit the scanning speed to get continuous lines by the overlap of single droplets. In this first printing, the energy is fixed and scanning speed varies from 600 mm/s to 100 mm/s. It is easy to understand that if the scanning speed is fast enough there will be no overlap and we will obtain single drops [4]. **FIG. 2** shows the result of several printings at different scanning speed. Single droplets are shown for fast scanning speed, whereas continuous lines are achieved by slowing the speed gradually. In first cases, the size of the drop is smaller than the distance between two absorption points, and this leads to a pair of droplets distinguishable. If the speed is reduced, these separated droplets will get closer and closer as the absorption points will become nearer. The objective is to overlap the droplets aiming to get a continuous conductive media. The obvious solution would be to scan at very slow speeds. Although this kind of procedure would lead to a first solution to the problem, getting a continuous conductive line, bulging [5] problem may appear. Higher resolution cannot be achieved in microelectronics if this phenomenon appears. Scanning at

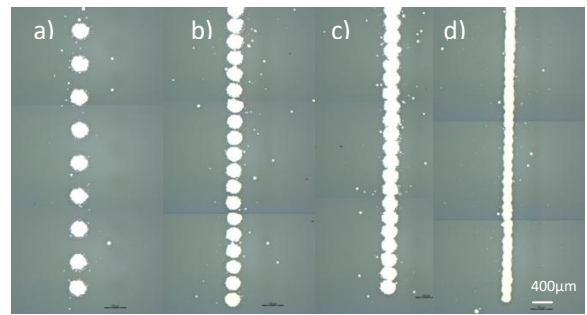


FIG. 2: Optical image of several printings with different scanning speeds. The energy per impulse corresponds to 0.2 mJ. The scanning speed corresponds to a) 600 mm/s b) 300 mm/s c) 250 mm/s d) 150 mm/s.

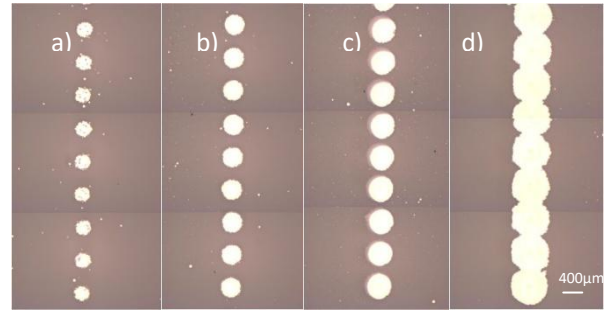


FIG. 3: Optical image of several printings with different energy printing. The scanning speed is 600 mm/s. The energy per impulse is a) 0.1 b) 0.2 c) 0.35 d) 0.7 mJ.

250 mm/s leads to our first conductive lines, as the droplets are all cohesive. Nevertheless, we decide to choose a slower speed at 150 mm/s. This is not an arbitrary choice, but to ensure the droplets are well overlapped. Comparing c) and d) in **FIG. 2**, they both are conductive, as their droplets are overlapped, but the faster one shows the single droplet contours, indicating a non regular line profile. For the contour to be regular, the droplets must be at least a 30% overlapped [5].

There is a strong relation between energy absorbed by the donor film and the material ejected to the acceptor substrate [6]. In this second printing it is necessary to observe the type of material transfer depending on the laser energy. It is shown in **FIG. 3** different droplets printed as the printing energy range changes. Printing at low energy shows the material deposition is small and irregular, as it is observed in the first image, corresponding to a 0.1 mJ energy supply. Increasing the energy to 0.2 mJ is enough to have a much better material deposition with a regular drop shape, as seen in the second image. If the energy keeps increasing, much more material is ejected and the droplets show irregularities in shape, as well as a lower resolution. Prove is shown in third and fourth images, corresponding to 0.35 and 0.7 mJ. The drops' size increases enough to even overlap with adjacent ones in consequence from the lost in resolution.

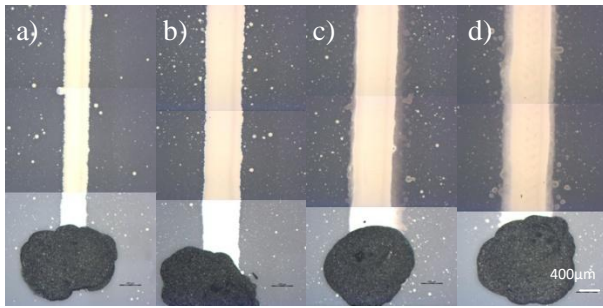


FIG. 4: Optical image of continuous conductive lines with different printing energy. The scanning speed is 150 mm/s. The energy per impulse is a) 0.1 b) 0.2 c) 0.35 d) 0.7 mJ.

It is important to choose wisely the printing energy of the laser. Not only the drops' shape matters, but also the dependence with the amount of ejected material, and in consequence, with the electrical resistance offered by the material. The energy range used in this third printing is the same as the previous one, and the scanning speed is now fixed to 150 mm/s. **FIG. 4** shows the results of the printing, corresponding to different energy lines. As the energy increases, the printed line becomes much wider and its contour starts becoming diffuse. Depending on the energy beam, three types of transfer dynamics can be distinguished [3,6]. The first one corresponds to low energy pulse beam, where the absorption of the laser pulse results in the formation of a bubble that expands, leading the flow of liquid along its walls, generating a higher pressure on its poles, where the liquid is released as a jet. This type corresponds to image a) shown in **FIG. 4** because of the low material ejected. This type of transfer would lead to the thinnest lines, but is very sensitive to the donor film uniformity and thickness. As the whole process of preparing the donor film is manually done, we cannot assure the repeatability of the experiment. Printing many times with the same experimental conditions (laser energy beam, ink volume deposited, spread surface, etc) has given different results. On one hand we get very thin conductive lines, but in the other hand gaps in the middle of the line appears, showing the non-uniformity of the material ejected. To prevent this fact, we decide to increase the energy beam and eject more material. The second type of transfer occurs when the energy is enough to break the bubbles' walls, creating

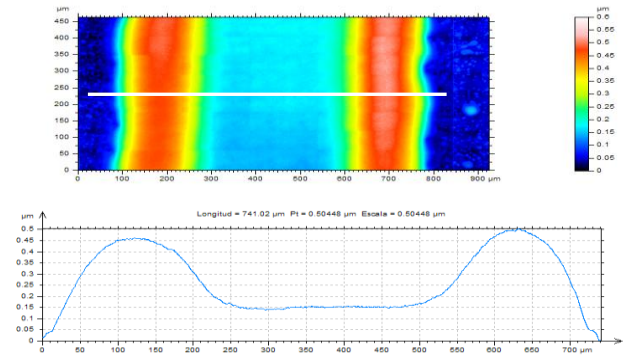


FIG. 5: Height profile for a printed line with energy per impulse of 0.2 mJ.

a burst before the jet can be formed. This would correspond to the second line printed, image b). In the transfer dynamics corresponding to the second process, the material ejected is no longer a jet, and the resolution decreases, but the reliability of the experiment is now assured. Finally, the third and last one transfer type is similar to the second one. The absorption of energy is great enough to break the bubbles walls, but it expands much faster, leading to contact the acceptor substrate before the burst happen. An increasing material deposition is observed, as well as a more irregular drop contour, as the third and fourth images show. The lines are no longer narrow, but liquid material splashed on the glass substrate with diffused contours.

As the resistivity is an intrinsic material property, and the discrepancy in length is negligible, the change in electrical resistance with the laser energy beam will be governed by the cross section of the line. The line width is measured with an optical microscopy, and the thickness is measured with confocal microscopy. **FIG. 5** shows the extracted line profiles with confocal microscopy. Accumulated material on both contours and a thinner central part is observed. This is known as the Marangoni effect or coffee ring [7]. During the drying process the central liquid material suffers a diffusion process towards the line sides, accumulating on the lateral extremes. It is observed that as the energy rises, the line becomes wider and the central thickness diminishes until the order of 70nm. This thickness corresponds to a few nanoparticles, getting a wide thin conductive film.

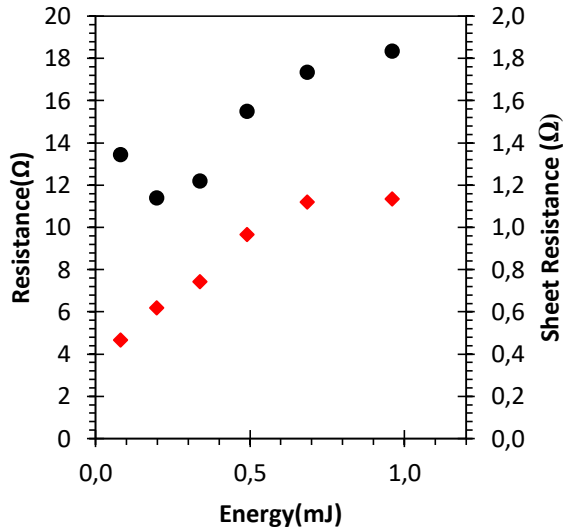


FIG. 6: Resistance ● and sheet resistance ◆ measured for different energy printings.

R Ω	E mJ	L mm ±0.1	w μm ±1	t nm ±10	Rs Ω	ρ Ω·cm ·1E-5
13.5±0.5	0.10	13.1	455	327	0.47	1.53
11.4±0.4	0.20	12.7	690	160	0.62	0.99
12.2±0.0	0.35	12.8	780	134	0.74	0.99
15.5±0.0	0.50	12.7	792	116	0.97	1.12
17.35±0.07	0.70	13.6	875	73	1.12	0.82
18.35±0.07	1.00	14.5	900	63	1.14	0.72

TABLE I. Data measured for resistance, energy, length, width, thickness, sheet resistance and resistivity.

The following question to answer is how the resistance varies with the laser power. **FIG. 6** shows the dependence measured in resistance for different laser energies. The increasing resistance with low energy seems understandable, as little material is ejected and the number of nanoparticles that are in contact decreases. In the limit, if the energy goes to zero, there would be no material and the resistance shall increase to infinity. Now higher energies are studied. Above the minimum resistance corresponding energy, the line geometry changes, as explained before, and we cannot relate the cross section with a rectangle, but something much complex. The central thickness decreases until we only have few nanoparticles, and the conduction capacity diminishes, increasing the resistance. Let us consider the sheet resistance

$$Rs = R \cdot \frac{w}{l} = \rho \cdot \frac{1}{t} \quad (1)$$

where w is the line width, R is the resistance, l is the line length, ρ the resistivity and t the thickness. Sheet resistance represents the resistance once we have removed the geometric effects, depending only in thickness. Once the geometry effects are corrected, the resistance-energy becomes linear increasing, a much easier dependence than the previous one. Using the profiles we measured with

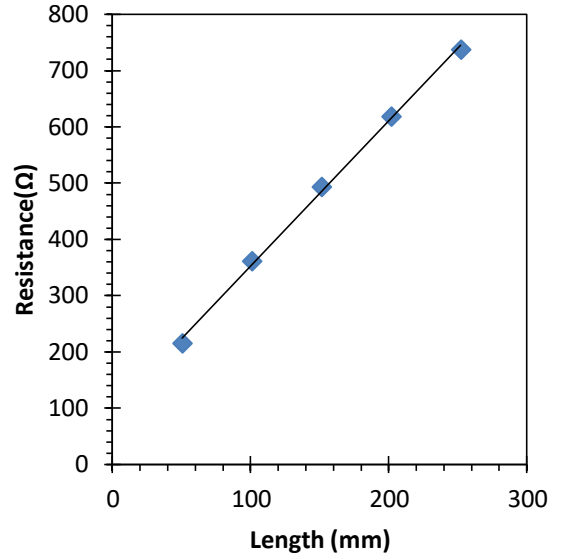


FIG. 7: Resistance measured for different path lengths.

confocal microscopy, and using the theoretical dependence of the sheet resistance with resistivity, approximating the cross section as a rectangle of surface

$$S = t \cdot w \quad (2)$$

we obtain an experimental value.

The experimental value obtained for the resistivity is chosen to be the average of the values we get in each line. Applying elemental statistics, we get $\rho = (10 \pm 3) \mu\Omega \cdot \text{cm}$. Compared to the nominal value, that corresponds to $\rho = 2 \mu\Omega \cdot \text{cm}$, the conductivity achieved is good but not the optimum, possibly affected by the irregular profile due to coffee ring effect or because the curing process was not done at the temperature specified in the technical sheet of the commercial silver. The results are summarized in **TABLE I**.

Finally, with the combination of the most appropriate scanning speed and the energy required for printing, a length study is done. It is necessary to characterize the length-resistance dependence, as we want to use these lines as wires in printed microelectronic circuits. The expected is to be linear, and if the length doubles, so will the resistance, as

$$R = \rho \frac{l}{t \cdot w} \quad (3)$$

FIG. 7 shows the linear dependence in length, but doubling length does not drive to a double resistance. To explain this phenomenon, line profiles need to be extracted to observe if the sample is uniform. The sample uniformity would lead to similar values of the resistance measures.

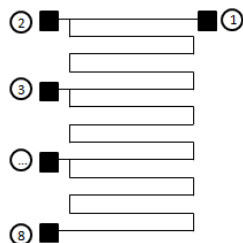


FIG. 8: Pattern printed to optimize the available surface to measure different lengths.

Electrodes	Resistance (Ω)
R34	215 \pm 10
R45	154 \pm 0.1
R56	144 \pm 0.1
R67	134 \pm 0.1
R78	128 \pm 0.1

TABLE II. Resistance measured for adjacent electrodes, to measure resistance for the same length.

	Top thickness (nm) \pm 10	Middle thickness (nm) \pm 10	Bottom thickness (nm) \pm 10
	196	271	372
	187	274	355
	-	244	351
Average thickness	191 \pm 5	263 \pm 5	359 \pm 5

TABLE III. Several line thicknesses measured for different positions of the sample.

The pattern design enables to measure the same length resistance in different parts of the substrate, as it is shown in **FIG. 8**. If the lines were uniform, the discrepancy in resistance would be very small, but the results show something different. Several adjacent electrodes are used to measure the same length resistance, and these values are posted in **TABLE II**. The decrease in resistance should come from a change in cross section, as the length is the same for each pair of electrodes. Moreover, the line width is pretty constant, so the reason must come from a change in thickness and, consequently, from a different absorption at the centre of the substrate. Using again confocal microscopy, several line profiles are scanned to get a thickness statistics. Effectively, the results came as expected as we can see in **TABLE III**. As the thickness

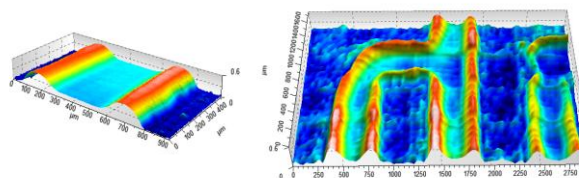


FIG. 9. 3D reconstructed images of a long line and a couple of right angle turns.

increases going from the top to the centre of the substrate, maintaining the width constant, the cross section grows and the resistance diminishes. As the line is not uniform along the entire sample, it explains the reason why doubling the length does not provoke a double resistance, but a smaller one. Some confocal images are shown in **FIG. 9** to prove the scope of technique. A line is scanned along 400 μ m to prove the possibilities that the LIFT technique can produce long conductive lines. The scanning shows the line non-uniformity, as it is clear it has also been affected by the Marangoni effect. A couple of right angles are shown to prove we can manufacture really complex patterns, opening a new field with new horizons to reach.

IV. CONCLUSIONS

The lines' conductivity is high even though they are not uniform because of the coffee ring effect during the drying process, or because of the curing process. Problems with non-uniformity of manufacturing the donor film forces us to use a higher energy to assure the printing success and, consequently, our printing resolution decreases. Finally, the resistance is proved to increase linearly despite the laser beam does not focus equally on both edges and the middle of the substrate. New strategies must be taken into account in order to correct these differences.

[1] A. Kamyshny, S. Magdassi, Conductive Nanomaterials for printed electronics. *Small*, 17, pp. 3515-3535, 2014.

[2] S. Khan, L. Lorenzelli and S.Dahiya. Technologies for Printing Sensors and Electronics Over Large Flexible Substrates: A Review. *IEEE Sensors Journal*, vol. 15, n° 6, pp. 3164-3165, 2015.

[3] J.M Fernández-Pradas, C. Florian, F. Caballero-Lucas, P. Sopeña, J.L. Morenza, P. Serra. Laser-induced forward transfer: Propelling liquids with light. *Appl. Surf. Sci.* 418, pp. 559-564, 2017.

[4] A. Palla-Papavlu, C. Córdoba, A. Patrascioiu, J.M. Fernández-Pradas, J.L. Morenza, P. Serra. Deposition and characterization of lines printed through laser-induced forward transfer. *Appl. Phys. A.*, 110: pp.751-755, 2013.

[5] C.Florian, F. Caballero-Lucas, J.M. Fernández-Pradas, R. Artigas, S. Ogier, D. Karnakis, P. Serra. Conductive silver ink printing through the laser-induced forward transfer dynamics. *Appl. Surf. Sci.*, 336, pp. 304-308, 2015.

[6] P. Sopeña, J.M. Fernández-Pradas, P. Serra. Laser-induced forward transfer of low viscosity inks. *Appl. Surf. Sci.*, 418, pp. 530-535, 2017.

[7] D. Sotman, V. Subramanian. Inkjet-Printed Line Morphologies and Temperature Control of the Coffee Ring Effect. *Langmuir*, 24, pp. 2224-2231, 2008.